Journal of Computational and Applied Mathematics 377 (2020) 112855

Contents lists available at ScienceDirect

Journal of Computational and Applied Mathematics

journal homepage: www.elsevier.com/locate/cam

Optimal rate convergence analysis of a second order scheme for a thin film model with slope selection

Shufen Wang [a], Wenbin Chen [b,*], Hanshuang Pan [a], Cheng Wang [c]

[a] School of Mathematical Sciences, Fudan University, Shanghai 200433, PR China
[b] School of Mathematical Sciences and Shanghai Key Laboratory for Contemporary Applied Mathematics, School of Mathematical Sciences, Fudan University, Shanghai 200433, PR China
[c] Department of Mathematics, University of Massachusetts, North Dartmouth, MA 02747, USA

ARTICLE INFO

Article history:
Received 28 April 2019
Received in revised form 25 February 2020

MSC:
35K55
65M12
65M60

Keywords:
Thin film epitaxy
Slope selection
Optimal rate convergence analysis
Mixed finite element
Preconditioned steepest descent solver

ABSTRACT

In this paper, an energy stable, second-order mixed finite element scheme is proposed and analyzed for the thin film epitaxial growth model with slope selection. We employ second-order backward differentiation formula (BDF) scheme with a second-order stabilized term, which guarantees the long time energy stability to approximate the continuous model. In terms of the convergence analysis, the key difficulty to derive an optimal rate spatial estimate is associated with the appearance of the gradient operator in the nonlinear terms, which may lead to a loss of optimal accuracy order. To overcome this well-known difficulty, we make use of some auxiliary techniques over triangular elements, and obtain an optimal convergence rate $\mathcal{O}(h^{q+1}+\Delta t^2)$, in comparison with $\mathcal{O}(h^{q}+\Delta t^2)$ rate from a standard projection estimate. Furthermore, we use an efficient preconditioned steepest descent (PSD) solver for the numerical implementation. A few numerical examples are presented to validate the stability and convergence.

1. Introduction

In this paper, we consider the thin film epitaxial growth model with slope selection(SS), which is the L^2 gradient flow of the following energy functional:

$$E(\phi)=\int_{\Omega}\left(\frac{1}{4}\left(|\nabla\phi|^2-1\right)^2+\frac{\varepsilon^2}{2}(\Delta\phi)^2\right)\mathrm{d}\mathbf{x}, \tag{1.1}$$

where $\Omega\subset\mathbb{R}^2$ is a convex polygon, $\phi=\phi(\mathbf{x},t)$ is a scaled height function of the thin film and ε is a given positive constant. The first term in $E(\phi)$ describes the Ehrlich–Schwoebel (ES) effect (see [1–3]), which gives the preference for the epitaxial films with slope satisfying $|\nabla\phi|\approx 1$, since this represents the minima of the first part. The second term depicts a surface diffusion effect, which will give the rounded corners in the film; a smaller value of ε corresponds to a sharper corner. It is widely believed that the energy E and the surface roughness R obey the scaling laws $E^{-1}\sim R\sim t^{1/3}$ (see [2,4]), and the saturation time scale is expected to be the order of ε^{-2} (see [5]). Only the 2D problems are studied here since the thin film model is mainly applied to the surface growth in practice. In fact, the analysis in this paper can be easily extended to the 3D case when needed.

* Corresponding author.
E-mail addresses: 17110180015@fudan.edu.cn (S. Wang), wbchen@fudan.edu.cn (W. Chen), 18210180017@fudan.edu.cn (H. Pan), cwang1@umassd.edu (C. Wang).

https://doi.org/10.1016/j.cam.2020.112855

The SS equation is the L^2 gradient flow associated with the energy $E(\phi)$, i.e., $\partial_t\phi = -\frac{\delta E}{\delta\phi}$, so that the height function ϕ satisfies

$$\begin{cases} \partial_t\phi + \nabla\cdot\left((1-|\nabla\phi|^2)\nabla\phi\right) - \varepsilon^2\Delta w = 0, & \text{in } \Omega\times(0,T], \\ w + \Delta\phi = 0, & \text{in } \Omega\times(0,T], \end{cases} \tag{1.2}$$

with exterior normal derivatives $\partial_n\phi = \partial_n w = 0$ on $\partial\Omega$ and the initial condition $\phi(\mathbf{x},0) = \phi_0(\mathbf{x})$ satisfying $(\phi_0, 1) \triangleq \int_\Omega \phi_0 d\mathbf{x} = 0$. Due to the Neumann boundary condition, this PDE system is mass conservative, namely, $(\phi, 1) = (w, 1) = 0$.

The corresponding weak form of system (1.2) turns out to be

$$\begin{cases} (\partial_t\phi, \varphi) + \varepsilon^2(\nabla w, \nabla\varphi) - \left((1-|\nabla\phi|^2)\nabla\phi, \nabla\varphi\right) = 0, & \text{in } \Omega\times(0,T], \\ (w, v) - (\nabla\phi, \nabla v) = 0, & \text{in } \Omega\times(0,T]. \end{cases} \tag{1.3}$$

There have been quite a few works focused on the numerical simulations for the SS equation in recent years. The primary challenge is associated with a proper discretization of the nonlinear term, as well as the long time energy stability. Two prevalent methods for this are the linear stabilization approach and the convex splitting approach. The former one treated the nonlinear term explicitly and added some linear stabilizing terms to improve stability. For example, a hybrid scheme was proposed in [6], which combines a high order backward differentiation for the time derivative and a high order extrapolation for the explicit treatment of the nonlinear term. A linear stabilization parameter A has to be sufficiently large to guarantee the energy dissipation law for this scheme. However, a theoretical justification of the lower bound for A has not been available until a recent work [7], in which the assumption on the boundedness of the numerical solution has been removed. This method has been widely adopted in a sequence of subsequent works [8–10] because of its simplicity. The second method splits the energy into convex and concave parts, and the two different parts are treated implicitly and explicitly, respectively. This method preserves an unconditional energy stability while the implicit treatment for the nonlinear terms gives rise to implementation difficulties. Besides application to the SS model with energy functional (1.1), the convex splitting method has been applied to solve the phase field crystal equation [5,11–16], the Cahn–Hilliard–Brinkman system [17–22], and the thin-film epitaxy model without slope selection [23–26], etc. Other methods for the SS equation, such as the operator splitting [27–29], the invariant energy quadratization [30,31] and the scalar auxiliary variable (SAV) approach [32], have also been successfully applied to the SS model. As for the spatial discretization, the spectral method is employed in [2,6], and the finite difference method has been analyzed in [33]. Semi-implicit time-stepping methods were proposed in [34,35] to solve the thin film epitaxy model (1.2), where the unconditional energy stability was established based on the convex splitting of the energy functional. In [36], a mixed finite element method and a backward Euler semi-implicit scheme with convex–concave decomposition of the nonlinear term were proposed. In addition, a combination of the mixed finite element method with Crank–Nicolson (CN) temporal discretization was reported in [37], in which the energy decay property was preserved due to the implicit treatment of the nonlinear term.

In particular, the second-order temporal convergence rate, combined with an $O(h^q)$ spatial convergence rate, was proved in [37]. Such a spatial accuracy comes from a standard projection estimate in the finite element space. On the other hand, one order higher accuracy has been observed in extensive numerical experiments. In this work, we provide a theoretical proof of the optimal convergence rate, $O(h^{q+1} + \Delta t^2)$, for the mixed finite element scheme combined with a second order BDF temporal discretization. Similar results for the thin film epitaxial growth model without slope selection (NSS) on regular rectangular mesh via the super-convergence theory have been presented in [38]. Moreover, this work was extended to quasi-uniform triangulation in [39] recently. The basic intuition came from the super-closeness property between the discrete solution and the Ritz projection of the continuous solution, see Lemma 2.2. While the application for such a skill to nonlinear equations is not trivial, some new techniques need to be introduced and the nonlinear terms should be handled carefully. In comparison, the nonlinearity in the NSS equation is relatively weak and the derivatives are uniformly bounded, thus the nonlinear terms can be treated explicitly. However, the boundedness is absent in the SS equation, for which the implicit treatment is required and there has been no improvement so far. In this article, the lack of boundedness will be overcome with the help of the Ritz projection and the convexity of the nonlinear terms owing to the implicit structure which plays an important role in the optimal convergence analysis.

Different from the NSS case considered in the recent work [39], in which the nonlinear terms are explicitly treated, therefore nonlinear iteration is not needed and it can be easily solved, the numerical implementation for the SS equation turns out to be highly challenging although the unique solvability and energy decay property have been proved for the CN scheme [34,37]. Such a difficulty comes from a subtle fact that there is no energy functional corresponding to the implicit terms appearing in the CN scheme. Because of such a non-symmetric feature of the nonlinear implicit terms, one could hardly make use of the convexity of the 4-Laplacian part, which may lead to a poor numerical performance in terms of computational efficiency. Regarding the nonlinear solver, a preconditioned steepest descent (PSD) algorithm, proposed in [40] to deal with regularized nonlinear elliptic equations, was considered in [33]. The PSD solver could be applied to many other nonlinear gradient models, in which the nonlinear terms correspond to a convex energy, such as the Cahn–Hilliard (CH) equation [41,42], the functionalized Cahn–Hilliard (FCH) equation [43,44], etc. In this work, we also apply the PSD solver for the numerical implementation. In particular, a geometric convergence analysis is available for such a nonlinear iteration. In our knowledge, no theoretical analysis has been available for the nonlinear solver involved in the CN scheme applied to the SS equation.

The rest of the paper is organized as follows. In Section 2, we propose the semidiscrete mixed finite element scheme for the system (1.3) and derive the corresponding error estimate. In Section 3, we apply a modified BDF2 algorithm to carry out the time discretization and provide the associated error estimate. Besides, the stability of this scheme is demonstrated, provided that the stabilized parameter $A \geq \frac{1}{16}$. The preconditioned steepest descent solver for the fully discrete scheme is outlined and the corresponding numerical results are shown in Section 4. In Section 5, we conclude the paper with a few remarks.

2. The semidiscrete scheme

In this section, we define the corresponding semidiscrete weak form to (1.2) and then derive the corresponding error estimate.

Following the notations in [45], we denote by $W^{m,p}(\Omega)$ and $H^m(\Omega)$ the Sobolev spaces, by $\|\cdot\|_{m,p}$ and $|\cdot|_{m,p}$ the standard norm and semi-norm respectively. For simplicity, $\|\cdot\|_{m,2}$ and $|\cdot|_{m,2}$ are written as $\|\cdot\|_m$ and $|\cdot|_m$, and the subscript is omitted when $m = 0$. Also we use $(\cdot, \cdot)$ to represent the L^2 inner product.

Given a positive constant $q \geq 1$, we define

$$L_0^2(\Omega) = \{u \in L^2(\Omega) \mid (u, 1) = 0\},$$
$$X = \{v \in H^1(\Omega) \mid (v, 1) = 0\}.$$

For the spatial discretization, we use quasi-uniform partition $\mathcal{T}_h$ on Ω with mesh grid size h. Upon this, the finite element space X_h is defined as

$$X_h = \{v \in X \cap C^0(\Omega) \;\big|\; v|_K \in \mathcal{P}_q(K),\ \forall K \in \mathcal{T}_h\},$$

with $\mathcal{P}_q$ the polynomials of degree not greater than q. In the semidiscrete problem, we also need to introduce Bochner space

$$L^2(0, T; X_h) = \left\{ v : (0, T) \to X_h,\ \|v\|_{L^2(0,T;X_h)} = \left(\int_0^T \|v(t)\|_{X_h}^2 \mathrm{d}t \right)^{1/2} < \infty \right\}.$$

The weak solution can be defined as follows.

Problem 2.1. Find $(\phi_h, w_h) \in L^\infty(0, T; X_h) \times L^2(0, T; X_h)$ and $\partial_t\phi_h \in L^2(0, T; X_h)$, such that for any $(\varphi_h, v_h) \in (X_h, X_h)$

$$\begin{cases} (\dfrac{\partial \phi_h}{\partial t}, \varphi_h) + \varepsilon^2(\nabla w_h, \nabla\varphi_h) - \big((1 - |\nabla\phi_h|^2)\nabla\phi_h, \nabla\varphi_h\big) = 0, & \forall t \in (0, T), \\ (w_h, v_h) - (\nabla\phi_h, \nabla v_h) = 0, & \forall t \in (0, T). \end{cases} \tag{2.1}$$

The unique solvability and energy stability for the semidiscrete system (2.1) have been proved in [37]. Specifically, the unique solvability was obtained by the eigenfunction expansion and a standard theory for ordinary differential equations. Besides, the energy identity is derived as:

$$\frac{d}{dt}E(\phi_h) + \|\partial_t\phi_h\|^2 = 0, \quad a.e.\ t \in (0, T).$$

In addition, an $\mathcal{O}(h^q)$ convergence rate was proved in [37]. In this section, we consider an optimal order error estimate, i.e., the same order of the interpolation approximation $\mathcal{O}(h^{q+1})$. Firstly, we define the Ritz projection $R_h : X \to X_h$ as

$$(\nabla R_h u, \nabla v_h) = (\nabla u, \nabla v_h), \quad \forall v_h \in X_h, \tag{2.2}$$

and the L^2 projection $P_h : X \to X_h$:

$$(P_h u, v_h) = (u, v_h), \quad \forall v_h \in X_h.$$

Moreover, the discrete Laplacian $\Delta_h : X_h \cap L_0^2 \to X_h \cap L_0^2$ is introduced as in [46, p. 10]: for any $\psi_h \in X_h \cap L_0^2$, let $\Delta_h\psi_h$ be the unique solution to

$$(\Delta_h\psi_h, \chi_h) = -(\nabla\psi_h, \nabla\chi_h), \quad \forall\chi_h \in X_h. \tag{2.3}$$

One has $\Delta_h R_h = P_h\Delta$ as shown in [46, p.11, (1.34)]. Recall the optimal $W^{1,p}$ estimate for the Ritz projection [47, p.101, Theorem A.2]:

Lemma 2.1. *Assume that Ω is a convex polygon and $\mathcal{T}_h$ is a quasi-uniform regular triangulation. Let $0 \leq s \leq q$ and $1 \leq p \leq \infty$ (when $q = 1$, then $2 \leq p < \infty$). There exists a constant $C > 0$, independent of h, such that the projection R_h satisfies the following error estimate:*

$$\|v - R_h v\|_{0,p} + h|v - R_h v|_{1,p} \leq Ch^{1+s}\|v\|_{s+1,p}, \quad \forall v \in W^{s+1,p}(\Omega).$$

Let ϕ and w be the exact solution pair to the original equations (1.2). Define

$$e_\phi \triangleq \rho_\phi + \sigma_\phi, \quad e_w \triangleq \rho_w + \sigma_w,$$
$$\text{with} \quad \rho_\phi = \phi - R_h\phi,\ \sigma_\phi = R_h\phi - \phi_h,\ \rho_w = w - R_h w,\ \sigma_w = R_h w - w_h.$$

Then we get the following error equations:

$$(\partial_t \sigma_\phi, \varphi_h) + \varepsilon^2(\nabla\sigma_w, \nabla\varphi_h) = -(\partial_t\rho_\phi, \varphi_h) + (\nabla\sigma_\phi, \nabla\varphi_h) + (|\nabla\phi_h|^2\nabla\phi_h - |\nabla\phi|^2\nabla\phi, \nabla\varphi_h), \tag{2.4}$$
$$(\sigma_w, v_h) - (\nabla\sigma_\phi, \nabla v_h) = -(\rho_w, v_h). \tag{2.5}$$

To establish the error estimate, we need an additional auxiliary technique about the super-closeness property between the discrete solution and the Ritz projection of the continuous solution. Its proof is referred to [39].

Lemma 2.2. *Given a real-valued function $a(\mathbf{x}) \in W^{1,\infty}(\Omega)$ (or $W^{1,\infty}(\Omega)^{2\times 2}$). Then ρ_ϕ and σ_ϕ satisfy*

$$(\nabla\rho_\phi, a(\mathbf{x})\nabla\sigma_\phi) \le C_1\|\Delta_h\sigma_\phi\|^2 + \frac{Ch^{2(q+1)}}{C_1}\|\phi\|_{q+1}^2,$$

in which C_1 is an arbitrary positive constant.

We denote by (ϕ, w) the exact solution pair to the original equation (1.3), then we say that the solution pair is of the regularity class $\mathcal{C}$ if and only if

$$\phi \in H^1(0,T;H^{q+1}) \cap L^2(0,T;W^{q+1,6}) \cap L^\infty(0,T;W^{2,\infty}), \tag{2.6}$$
$$w \in L^2(0,T;H^{q+1}), \tag{2.7}$$

and the solution pair is of the regularity class $\mathcal{C}_1$ if and only if

$$\begin{aligned} &\phi \in L^\infty(0,T;W^{2,\infty}) \cap L^\infty(0,T;W^{q+1,6}) \cap H^1(0,T;H^{q+1}) \cap W^{2,\infty}(0,T;L^2) \\ &\quad \cap W^{1,\infty}(0,T;H^2) \cap H^3(0,T;L^2) \cap H^2(0,T;H^1), \\ &w \in L^\infty(0,T;H^{q+1}) \cap H^1(0,T;H^{q+1}). \end{aligned} \tag{2.8}$$

Next, we provide an optimal error estimate for the semidiscrete scheme.

Theorem 2.2. *Let (ϕ, w) be the solution of (1.3) in the regularity class $\mathcal{C}$. Then the finite element approximation (ϕ_h, w_h) of (2.1) with $\phi_h(x,0) = R_h\phi(x,0)$ has the following error estimate*

$$\|\phi(x,T) - \phi_h(x,T)\|^2 + \int_0^T \|w - w_h\|^2 dt \le C_{\varepsilon,T}h^{2q+2}, \tag{2.9}$$

where $C_{\varepsilon,T}$ is a constant that only depends on ε and T.

Proof. Let $\varphi_h = \sigma_\phi$ in (2.4), $v_h = \varepsilon^2\Delta_h\sigma_\phi$ in (2.5) and add up the two equations

$$\frac{1}{2}\frac{d}{dt}\|\sigma_\phi\|^2 + \varepsilon^2\|\Delta_h\sigma_\phi\|^2 = \|\nabla\sigma_\phi\|^2 - (\partial_t\rho_\phi, \sigma_\phi) - \varepsilon^2(\rho_w, \Delta_h\sigma_\phi) + \mathcal{N}_1 + \mathcal{N}_2, \tag{2.10}$$

where

$$\mathcal{N}_1 = (|\nabla\phi_h|^2\nabla\phi_h - |\nabla R_h\phi|^2\nabla R_h\phi, \nabla\sigma_\phi),$$
$$\mathcal{N}_2 = (|\nabla R_h\phi|^2\nabla R_h\phi - |\nabla\phi|^2\nabla\phi, \nabla\sigma_\phi).$$

Using the Young's inequality for $\mathcal{N}_1$:

$$\begin{aligned} \mathcal{N}_1 &= \left(|\nabla\phi_h|^2\nabla\phi_h, \nabla R_h\phi - \nabla\phi_h\right) - \left(|\nabla R_h\phi|^2\nabla R_h\phi, \nabla R_h\phi - \nabla\phi_h\right) \\ &= -\|\nabla\phi_h\|_{0,4}^4 - \|\nabla R_h\phi\|_{0,4}^4 + \left(|\nabla\phi_h|^2\nabla\phi_h, \nabla R_h\phi\right) + \left(|\nabla R_h\phi|^2\nabla R_h\phi, \nabla\phi_h\right) \\ &\le -\frac{1}{2}\|\nabla\phi_h\|_{0,4}^4 - \frac{1}{2}\|\nabla R_h\phi\|_{0,4}^4 + \left(|\nabla R_h\phi|^2, |\nabla\phi_h|^2\right) \\ &\le 0. \end{aligned} \tag{2.11}$$

To estimate $\mathcal{N}_2$, we first split it into two parts

$$\begin{aligned} \mathcal{N}_2 &= \left((\nabla R_h\phi - \nabla\phi)|\nabla\phi|^2, \nabla\sigma_\phi\right) + \left((|\nabla R_h\phi|^2 - |\nabla\phi|^2)\nabla R_h\phi, \nabla\sigma_\phi\right) \\ &:= \Pi_1 + \Pi_2. \end{aligned} \tag{2.12}$$

Note that $|\nabla\phi|^2 \in W^{1,\infty}(\Omega)$ for ϕ in the regularity class $\mathcal{C}$. Applying Lemma 2.2, one gets

$$|\Pi_1| \le C_1\|\Delta_h\sigma_\phi\|^2 + \frac{Ch^{2q+2}}{C_1}\|\phi\|_{q+1}^2. \tag{2.13}$$

Subsequently, split Π_2 into four parts:

$$\begin{aligned}\Pi_2 &= \big((|\nabla R_h\phi|^2 - |\nabla\phi|^2)\nabla R_h\phi, \nabla\sigma_\phi\big)\\ &= \big(\nabla\rho_\phi\cdot(-\nabla\rho_\phi + 2\nabla\phi)(-\nabla\rho_\phi + \nabla\phi), \nabla\sigma_\phi\big)\\ &= (\nabla\rho_\phi(\nabla\rho_\phi)^T\nabla\rho_\phi, \nabla\sigma_\phi) + 2(\nabla\rho_\phi(\nabla\phi)^T\nabla\rho_\phi, \nabla\sigma_\phi)\\ &\quad + (\nabla\phi(\nabla\rho_\phi)^T\nabla\rho_\phi, \nabla\sigma_\phi) + 2(\nabla\phi(\nabla\phi)^T\nabla\rho_\phi, \nabla\sigma_\phi)\\ &:= \text{(I)} + \text{(II)} + \text{(III)} + \text{(IV)}.\end{aligned} \tag{2.14}$$

Using Hölder's inequality and Lemma 2.1, one obtains

$$|\text{(I)}| \le \|\nabla\rho_\phi\|_{0,6}^3\|\nabla\sigma_\phi\| \le C_2\|\nabla\sigma_\phi\|^2 + \frac{C}{C_2}h^{6q}\|\phi\|_{q+1,6}^6. \tag{2.15}$$

Similar estimates could also be derived:

$$\begin{aligned}|\text{(II)}| &\le C\|\phi\|_{1,\infty}\|\nabla\rho_\phi\|_{0,4}^2\|\nabla\sigma_\phi\| \le C_2\|\nabla\sigma_\phi\|^2 + \frac{C}{C_2}h^{4q}\|\phi\|_{q+1,4}^4,\\ |\text{(III)}| &\le C\|\phi\|_{1,\infty}\|\nabla\rho_\phi\|_{0,4}^2\|\nabla\sigma_\phi\| \le C_2\|\nabla\sigma_\phi\|^2 + \frac{C}{C_2}h^{4q}\|\phi\|_{q+1,4}^4.\end{aligned} \tag{2.16}$$

Since a simple calculation shows that $\nabla\phi(\nabla\phi)^T \in W^{1,\infty}(\Omega)^{2\times 2}$, an application of Lemma 2.2 leads to

$$|\text{(IV)}| \le C_1\|\Delta_h\sigma_\phi\|^2 + \frac{C}{C_1}h^{2q+2}\|\phi\|_{q+1}^2. \tag{2.17}$$

A substitution of (2.11)–(2.17) into (2.10) yields

$$\begin{aligned}\frac{1}{2}\frac{d}{dt}\|\sigma_\phi\|^2 + \frac{\varepsilon^2}{2}\|\Delta_h\sigma_\phi\|^2 &\le C\varepsilon^2h^{2q+2}\|w\|_{q+1}^2 + C_3\|\sigma_\phi\|^2 + \frac{C}{C_3}h^{2q+2}\|\phi_t\|_{q+1}^2\\ &\quad + (1+3C_2)\|\nabla\sigma_\phi\|^2 + 2C_1\|\Delta_h\sigma_\phi\|^2 + \frac{C}{C_1}h^{2q+2}\|\phi\|_{q+1}^2\\ &\quad + \frac{C}{C_2}h^{6q}\|\phi\|_{q+1,6}^6 + \frac{C}{C_2}h^{4q}\|\phi\|_{q+1,4}^4.\end{aligned} \tag{2.18}$$

Also notice that

$$\|\nabla\sigma_\phi\|^2 = -(\sigma_\phi, \Delta_h\sigma_\phi) \le \frac{\varepsilon^2}{4}\|\Delta_h\sigma_\phi\|^2 + \frac{1}{\varepsilon^2}\|\sigma_\phi\|^2. \tag{2.19}$$

By taking $C_1 = \frac{\varepsilon^2}{32}$, $C_2 = \frac{1}{12}$, an application of Gronwall inequality gives

$$\begin{aligned}\|\sigma_\phi(x,T)\|^2 + \int_0^T \frac{\varepsilon^2}{4}\|\Delta_h\sigma_\phi\|^2 \mathrm{dt} &\le C_\varepsilon\bigg(h^{2q+2}\int_0^T(\|w\|_{q+1}^2 + \|\phi_t\|_{q+1}^2 + \|\phi\|_{q+1}^2)\mathrm{dt}\\ &\quad + \int_0^T(h^{6q}\|\phi\|_{q+1,6}^6 + h^{4q}\|\phi\|_{q+1,4}^4)\mathrm{dt}\bigg).\end{aligned} \tag{2.20}$$

Note that $\phi_h(x,0) = R_h\phi(x,0)$ has been used to eliminate the term $\sigma_\phi(x,0)$, then we arrive at the estimate for e_ϕ.

As for e_w, by the second equation of (2.1) and the relationship between P_h and R_h, i.e., $\Delta_h R_h = P_h\Delta$, one gets,

$$\begin{aligned}\|e_w\| &= \|(I-P_h)w + P_h\Delta\phi - \Delta_h\phi_h\| = \|(I-P_h)w + \Delta_h\sigma_\phi\|\\ &\le \|(I-P_h)w\| + \|\Delta_h\sigma_\phi\|.\end{aligned}$$

The estimate for e_w then follows from the approximation property of the L^2-orthogonal projection and (2.20). This completes the proof of Theorem 2.2. □

Remark 2.1. Unlike the results in [37], in which only an $\mathcal{O}(h^q)$ convergence order was proved (due to the nonlinear estimates), we obtain an $\mathcal{O}(h^{q+1})$ convergence order. The key point of this improved analysis is to establish a super-closeness estimate between the discrete solution and the Ritz projection of the continuous solution. Similar techniques have also been reported in recent works [39,48].

Remark 2.2. In the estimation (2.11) for nonlinear term $\mathcal{N}_1$, the convexity of the 4-Laplacian part is crucial and greatly simplifies our analysis. The form of the nonlinear terms in the NSS equation was more complex and the boundedness played the major role in the error estimation in [39].

3. The fully discrete scheme

In this section, we use the BDF2 algorithm to carry out the temporal discretization over the time interval $[0, T]$. Given a positive integer N, let $\Delta t = T/N$ be the uniform time step size and denote by, $t_n = n\Delta t,\ 0 \le n \le N$, the nodes. Then a fully discrete error estimate is provided. In addition, the energy decay property of the fully discrete scheme is proved, in terms of a modified energy functional, and an efficient iterative algorithm is presented to implement the numerical scheme. The BDF2 method has already been successfully applied to the CH equation [49,50], as well as the variable time step size version [51]. An application of a modified BDF2 algorithm to the SS equation was first reported in [33], with finite difference spatial approximation.

The use of BDF2 approximation leads to the following fully discrete problem.

Problem 3.1. Given $(\phi_h^n, w_h^n) \in X_h \times X_h$, find $(\phi_h^{n+1}, w_h^{n+1}) \in X_h \times X_h$ such that for arbitrary $(\varphi_h, \upsilon_h) \in X_h \times X_h$

$$\begin{cases} \left(\dfrac{3\phi_h^{n+1} - 4\phi_h^n + \phi_h^{n-1}}{2\Delta t}, \varphi_h\right) + \varepsilon^2(\nabla w_h^{n+1}, \nabla\varphi_h) + A\Delta t\big(\nabla(w_h^{n+1} - w_h^n), \nabla\varphi_h\big) \\ \qquad + (|\nabla\phi_h^{n+1}|^2\nabla\phi_h^{n+1}, \nabla\varphi_h) - \big(\nabla(2\phi_h^n - \phi_h^{n-1}), \nabla\varphi_h\big) = 0, \\ (w_h^{n+1}, \upsilon_h) - (\nabla\phi_h^{n+1}, \nabla\upsilon_h) = 0, \end{cases} \tag{3.1}$$

where $A \ge \frac{1}{16}$ is a given constant. At the initial step t_1, let $\phi_h^0 = R_h\phi_0$, $w_h^0 = R_h(-\Delta\phi_0)$, we set

$$\begin{cases} \left(\dfrac{\phi_h^1 - \phi_h^0}{\Delta t}, \varphi_h\right) + \varepsilon^2(\nabla w_h^1, \nabla\varphi_h) + (|\nabla\phi_h^1|^2\nabla\phi_h^1, \nabla\varphi_h) - (\nabla\phi_h^0, \nabla\varphi_h) = 0, \\ (w_h^1, \upsilon_h) - (\nabla\phi_h^1, \nabla\upsilon_h) = 0. \end{cases} \tag{3.2}$$

In [37], a modified CN approximation was employed to the temporal discretization for (2.1). The existence of the solution was proved by the Brouwer fixed-point theorem and its combination with the property of the continuous dependence on the initial value led to the unique solvability analysis. The corresponding discrete energy identity became

$$E(\phi_h^{n+1}) - E(\phi_h^n) = -\Delta t \left\| \frac{\phi_h^{n+1} - \phi_h^n}{\Delta t} \right\|^2, \quad \forall n \ge 0.$$

Meanwhile, an $\mathcal{O}(h^q + \Delta t^2)$ accurate order error estimate was proved in [37]. For the BDF2 scheme presented in this section, we can easily obtain the unique solvability owing to the convex nature of the implicit terms, and the similar analysis has already been given in [38,50]. Additionally, a modified energy stability can be obtained using a careful energy analysis. More importantly, an optimal convergence rate $\mathcal{O}(h^{q+1} + \Delta t^2)$ will be established via the super-closeness theory.

Lemma 3.1. *The fully discrete scheme 3.1 has a unique solution.*

3.1. Energy stability

First, we consider the energy stability for the initial step. We introduce a discrete energy which is consistent with the continuous space energy as $h \to 0$:

$$E(\phi_h^{n+1}, w_h^{n+1}) = \frac{1}{4}\|\nabla\phi_h^{n+1}\|_{0,4}^4 - \frac{1}{2}\|\nabla\phi_h^{n+1}\|^2 + \frac{\varepsilon^2}{2}\|w_h^{n+1}\|^2. \tag{3.3}$$

Initial energy decay, $E(\phi_h^1, w_h^1) \le E(\phi_h^0, w_h^0)$, could be proved, while such a property is not available for $n \ge 1$. We define a modified energy for the analysis:

$$\widetilde{E}(\phi_h^{n+1}, w_h^{n+1}) = E(\phi_h^{n+1}, w_h^{n+1}) + \frac{1}{4\Delta t}\|\phi_h^{n+1} - \phi_h^n\|^2 + \frac{1}{2}\|\nabla(\phi_h^{n+1} - \phi_h^n)\|^2. \tag{3.4}$$

Theorem 3.2. *The discrete energy $E(\phi_h^n, w_h^n)$ decays at the initial step. And also, the modified energy $\widetilde{E}(\phi_h^n, w_h^n)$ has the following decay property:*

$$\widetilde{E}(\phi_h^{n+1}, w_h^{n+1}) \le \widetilde{E}(\phi_h^n, w_h^n), \quad \forall n \ge 1, \tag{3.5}$$

provided that $A \ge \frac{1}{16}$.

Proof. Taking $\varphi_h = \phi_h^1 - \phi_h^0$ in the first equality of (3.2) yields

$$
\begin{aligned}
0 &= \frac{\|\phi_h^1 - \phi_h^0\|^2}{\Delta t} + \varepsilon^2\big(\nabla w_h^1, \nabla(\phi_h^1 - \phi_h^0)\big) \\
&\quad - \big(\nabla \phi_h^0, \nabla(\phi_h^1 - \phi_h^0)\big) + \big(|\nabla \phi_h^1|^2 \nabla \phi_h^1, \nabla(\phi_h^1 - \phi_h^0)\big) \\
&\geq \frac{\|\phi_h^1 - \phi_h^0\|^2}{\Delta t} + \frac{\varepsilon^2}{2}(\|w_h^1\|^2 - \|w_h^0\|^2) + \frac{\|\nabla \phi_h^0\|^2 - \|\nabla \phi_h^1\|^2}{2} + \frac{\|\nabla \phi_h^1\|_{0,4}^4 - \|\nabla \phi_h^0\|_{0,4}^4}{4},
\end{aligned}
\tag{3.6}
$$

which leads to

$$
E(\phi_h^1, w_h^1) - E(\phi_h^0, w_h^0) \leq -\frac{\|\phi_h^1 - \phi_h^0\|^2}{\Delta t} \leq 0. \tag{3.7}
$$

As for $n \geq 1$, taking $\varphi_h = \phi_h^{n+1} - \phi_h^n$ in the first equation of (3.1):

$$
\begin{aligned}
0 &= \left(\frac{3\phi_h^{n+1} - 4\phi_h^n + \phi_h^{n-1}}{2\Delta t}, \phi_h^{n+1} - \phi_h^n\right) + \varepsilon^2\big(\nabla w_h^{n+1}, \nabla(\phi_h^{n+1} - \phi_h^n)\big) \\
&\quad + A\Delta t\big(\nabla(w_h^{n+1} - w_h^n), \nabla(\phi_h^{n+1} - \phi_h^n)\big) + \big(|\nabla \phi_h^{n+1}|^2 \nabla \phi_h^{n+1}, \nabla(\phi_h^{n+1} - \phi_h^n)\big) \\
&\quad - \big(\nabla(2\phi_h^n - \phi_h^{n-1}), \nabla(\phi_h^{n+1} - \phi_h^n)\big) \\
&:= \mathrm{I}_1 + \mathrm{I}_2 + \mathrm{I}_3 + \mathrm{I}_4 + \mathrm{I}_5.
\end{aligned}
\tag{3.8}
$$

An application of the Cauchy–Schwarz inequality gives a direct estimate for I_1:

$$
\mathrm{I}_1 \geq \frac{1}{\Delta t}\Big(\frac{5}{4}\|\phi_h^{n+1} - \phi_h^n\|^2 - \frac{1}{4}\|\phi_h^n - \phi_n^{n-1}\|^2\Big). \tag{3.9}
$$

Likewise, I_4 and I_5 have the following lower bounds:

$$
\mathrm{I}_4 = \|\nabla \phi_h^{n+1}\|_{0,4}^4 - (|\nabla \phi_h^{n+1}|^2 \nabla \phi_h^{n+1}, \nabla \phi_h^n) \geq \frac{1}{4}\big(\|\nabla \phi_h^{n+1}\|_{0,4}^4 - \|\nabla \phi_h^n\|_{0,4}^4\big), \tag{3.10}
$$

$$
\begin{aligned}
\mathrm{I}_5 &= (-\nabla \phi_h^n, \nabla \phi_h^{n+1} - \nabla \phi_h^n) - (\nabla \phi_h^n - \nabla \phi_h^{n-1}, \nabla \phi_h^{n+1} - \nabla \phi_h^n) \\
&= \frac{1}{2}\|\nabla \phi_h^{n+1} - \nabla \phi_h^n\|^2 + \frac{1}{2}\|\nabla \phi_h^n\|^2 - \frac{1}{2}\|\nabla \phi_h^{n+1}\|^2 \\
&\quad - \big(\nabla(\phi_h^n - \phi_h^{n-1}), \nabla(\phi_h^{n+1} - \phi_h^n)\big) \\
&\geq -\frac{1}{2}(\|\nabla \phi_h^{n+1}\|^2 - \|\nabla \phi_h^n\|^2) - \frac{1}{2}\|\nabla(\phi_h^n - \phi_h^{n-1})\|^2.
\end{aligned}
\tag{3.11}
$$

For I_2, we employ the second part of (3.1) as well as the Cauchy–Schwarz inequality

$$
\mathrm{I}_2 \geq \frac{\varepsilon^2}{2}\big(\|w_h^{n+1}\|^2 - \|w_h^n\|^2\big). \tag{3.12}
$$

In addition, making use of (2.3), the artificial term can be handled in the same manner

$$
\begin{aligned}
\mathrm{I}_3 + \frac{1}{\Delta t}\|\phi_h^{n+1} - \phi_h^n\|^2 &= A\Delta t\|\Delta_h(\phi_h^{n+1} - \phi_h^n)\|^2 + \frac{1}{\Delta t}\|\phi_h^{n+1} - \phi_h^n\|^2 \\
&\geq 2\sqrt{A}\|\nabla(\phi_h^{n+1} - \phi_h^n)\|^2.
\end{aligned}
\tag{3.13}
$$

Therefore, a combination of (3.8)–(3.13) results in

$$
\begin{aligned}
&E(\phi_h^{n+1}, w_h^{n+1}) - E(\phi_h^n, w_h^n) + \frac{1}{4}\|\phi_h^{n+1} - \phi_h^n\|^2 - \frac{1}{4}\|\phi_h^n - \phi_h^{n-1}\|^2 \\
&\quad + \frac{1}{2}\|\nabla(\phi_h^{n+1} - \phi_h^n)\|^2 - \frac{1}{2}\|\nabla(\phi_h^n - \phi_h^{n-1})\|^2 \\
&\leq (\frac{1}{2} - 2\sqrt{A})\|\nabla(\phi_h^{n+1} - \phi_h^n)\|^2 \leq 0,
\end{aligned}
\tag{3.14}
$$

provided that $A \geq \frac{1}{16}$. This completes the proof of Theorem 3.2, upon the definition of $\widetilde{E}$. □

Remark 3.1. In [52], a stabilization of the form $-A\Delta(\phi^{n+1} - 2\phi^n + \phi^{n-1})$ was considered and analyzed for the 2D CH equation with the nonlinear term explicitly treated by an extrapolation, for which the unconditional energy stability independent of the time step size Δt was proved therein and the stabilization parameter A depends on the interface width ε. The anonymous reviewer indicates that a similar idea could also be applied for the SS equation in the 2D case. Such a technique will lead to a total linear system and a more stringent condition depending on the interface parameter for the stabilized coefficient may be required, which could be considered in the future.

Based on the energy stability, we are able to derive the $L^\infty(0,T;H^2)$ stability of the numerical solution.

Lemma 3.2. *If $(\phi_h^{n+1}, w_h^{n+1})$ is the solution of Problem 3.1, then we have the following bound:*

$$E(\phi_h^{n+1}, w_h^{n+1}) \le C_0, \qquad \varepsilon^2 \|\Delta_h \phi_h^{n+1}\|^2 \le 2(C_0 + |\Omega|), \quad \forall n \ge 0, \tag{3.15}$$

in which C_0 is independent of step size Δt, h and final time T.

Proof. Theorem 3.2 implies that $\widetilde{E}(\phi_h^{n+1}, w_h^{n+1}) \le \widetilde{E}(\phi_h^n, w_h^n)$, inductively

$$\begin{aligned} &E(\phi_h^{n+1}, w_h^{n+1}) \le \widetilde{E}(\phi_h^{n+1}, w_h^{n+1}) \\ \le\ & E(\phi_h^0, w_h^0) + \frac{1}{4\Delta t}\|\phi_h^1 - \phi_h^0\|^2 + \frac{1}{2}\|\nabla(\phi_h^1 - \phi_h^0)\|^2 \\ \le\ & E(\phi_h^0, w_h^0) + \frac{1}{4\Delta t}\|\phi_h^1 - \phi_h^0\|^2 + \|\nabla\phi_h^1\|^2 + \|\nabla\phi_h^0\|^2. \end{aligned} \tag{3.16}$$

On the other hand, a simple calculation shows that

$$\frac{1}{8}u^4 - \frac{1}{2}u^2 \ge -\frac{1}{2},$$

which in turn leads to

$$\frac{1}{8}\|\nabla\phi_h\|_{0,4}^4 - \frac{1}{2}\|\nabla\phi_h\|^2 \ge -\frac{1}{2}|\Omega|.$$

In combination with the definition of discrete energy (3.3), one gets

$$\begin{aligned} E(\phi_h^0, w_h^0) \ge E(\phi_h^1, w_h^1) &\ge \frac{1}{8}\|\nabla\phi_h^1\|_{0,4}^4 + \frac{\varepsilon^2}{2}\|w_h^1\|^2 - \frac{1}{2}|\Omega| \\ &\ge \frac{1}{2}\|\nabla\phi_h^1\|^2 + \frac{\varepsilon^2}{2}\|w_h^1\|^2 - |\Omega|, \end{aligned} \tag{3.17}$$

which gives a bound of $\|\nabla\phi_h^1\|^2$. And from (3.6) we know that $\|\phi_h^1 - \phi_h^0\|^2/\Delta t$ can be bounded by a constant from above. Going back to Eq. (3.16), one gets $E(\phi_h^{n+1}, w_h^{n+1}) \le C_0$. Meanwhile, a similar inequality as (3.17) could be derived:

$$\begin{aligned} E(\phi_h^{n+1}, w_h^{n+1}) &\ge \frac{1}{8}\|\nabla\phi_h^{n+1}\|_{0,4}^4 + \frac{\varepsilon^2}{2}\|w_h^{n+1}\|^2 - \frac{1}{2}|\Omega| \\ &\ge \frac{1}{2}\|\nabla\phi_h^{n+1}\|^2 + \frac{\varepsilon^2}{2}\|w_h^{n+1}\|^2 - |\Omega| \\ &\ge \frac{\varepsilon^2}{2}\|\Delta_h\phi_h^{n+1}\|^2 - |\Omega|, \end{aligned} \tag{3.18}$$

in which (2.3) and (3.1) have been used in the last step. This completes the proof of Lemma 3.2. □

3.2. The optimal error estimate

In this subsection we deal with the optimal error estimate of the fully discrete system in Problem 3.1. The corresponding error equations for $n \ge 1$ become

$$\begin{aligned} &(\delta_{\Delta t}^{n+1}\sigma_\phi, \varphi_h) + \varepsilon^2(\nabla\sigma_w^{n+1}, \nabla\varphi_h) + A\Delta t\big(\nabla(\sigma_w^{n+1} - \sigma_w^n), \nabla\varphi_h\big) \\ &\quad = \big(\nabla(2\sigma_\phi^n - \sigma_\phi^{n-1}), \nabla\varphi_h\big) - (\delta_{\Delta t}^{n+1}\rho_\phi, \varphi_h) + (\mathcal{R}_1^{n+1}, \varphi_h) + A\Delta t(\mathcal{R}_2^{n+1}, \nabla\varphi_h) \\ &\qquad + (\mathcal{R}_3^{n+1}, \nabla\varphi_h) + (\mathcal{N}_1^{n+1}, \nabla\varphi_h) + (\mathcal{N}_2^{n+1}, \nabla\varphi_h), \end{aligned} \tag{3.19}$$

$$(\sigma_w^{n+1}, v_h) - (\nabla\sigma_\phi^{n+1}, \nabla v_h) = -(\rho_w^{n+1}, v_h), \tag{3.20}$$

where

$$\begin{aligned} &\delta_{\Delta t}^{n+1}u = \frac{3u^{n+1} - 4u^n + u^{n-1}}{2\Delta t}, \qquad \mathcal{R}_1^{n+1} = \delta_{\Delta t}^{n+1}\phi - \phi_t^{n+1}, \\ &\mathcal{R}_2^{n+1} = \nabla(w^{n+1} - w^n), \qquad \mathcal{R}_3^{n+1} = \nabla(\phi^{n+1} - 2\phi^n + \phi^{n-1}), \\ &\mathcal{N}_1^{n+1} = |\nabla\phi_h^{n+1}|^2\nabla\phi_h^{n+1} - |\nabla R_h\phi^{n+1}|^2\nabla R_h\phi^{n+1}, \\ &\mathcal{N}_2^{n+1} = |\nabla R_h\phi^{n+1}|^2\nabla R_h\phi^{n+1} - |\nabla\phi^{n+1}|^2\nabla\phi^{n+1}. \end{aligned}$$

And for $n=0$, one has

$$\Big(\frac{\sigma_\phi^1-\sigma_\phi^0}{\Delta t},\varphi_h\Big)+\varepsilon^2(\nabla\sigma_w^1,\nabla\varphi_h)-(\nabla\sigma_\phi^0,\nabla\varphi_h)+(\nabla\phi^1-\nabla\phi^0,\nabla\varphi_h)$$
$$=-\Big(\frac{\rho_\phi^1-\rho_\phi^0}{\Delta t},\varphi_h\Big)+\Big(\frac{\phi^1-\phi^0}{\Delta t}-\phi_t^1,\varphi_h\Big)+(\mathcal{N}_1^1,\nabla\varphi_h)+(\mathcal{N}_2^1,\nabla\varphi_h), \tag{3.21}$$
$$(\sigma_w^1,v_h)-(\nabla\sigma_\phi^1,\nabla v_h)=-(\rho_w^1,v_h), \tag{3.22}$$

with

$$\mathcal{N}_1^1=|\nabla\phi_h^1|^2\nabla\phi_h^1-|\nabla R_h\phi^1|^2\nabla R_h\phi^1,\qquad \mathcal{N}_2^1=|\nabla R_h\phi^1|^2\nabla R_h\phi^1-|\nabla\phi^1|^2\nabla\phi^1.$$

First we consider the case for $n\geq 1$. Taking $\varphi_h=\sigma_\phi^{n+1}$ in (3.19), $v_h=\varepsilon^2\Delta_h\sigma_\phi^{n+1}$ in (3.20) and adding up the two equations lead to

$$\begin{aligned}&(\delta_{\Delta t}^{n+1}\sigma_\phi,\sigma_\phi^{n+1})+\varepsilon^2\|\Delta_h\sigma_\phi^{n+1}\|^2+A\Delta t\big(\nabla(\sigma_w^{n+1}-\sigma_w^n),\nabla\sigma_\phi^{n+1}\big)\\ &=\big(\nabla(2\sigma_\phi^n-\sigma_\phi^{n-1}),\nabla\sigma_\phi^{n+1}\big)-(\delta_{\Delta t}^{n+1}\rho_\phi,\sigma_\phi^{n+1})+(\mathcal{R}_1^{n+1},\sigma_\phi^{n+1})\\ &\quad+A\Delta t(\mathcal{R}_2^{n+1},\nabla\sigma_\phi^{n+1})+(\mathcal{R}_3^{n+1},\nabla\sigma_\phi^{n+1})\\ &\quad-\varepsilon^2(\rho_w^{n+1},\Delta_h\sigma_\phi^{n+1})+(\mathcal{N}_1^{n+1}+\mathcal{N}_2^{n+1},\nabla\sigma_\phi^{n+1}).\end{aligned} \tag{3.23}$$

It is now easy to show that $(\mathcal{N}_1^{n+1},\nabla\sigma_\phi^{n+1})$ is less than zero on the basis of (2.11) . Besides, the estimate (2.12) implies that

$$\begin{aligned}|(\mathcal{N}_2^{n+1},\nabla\sigma_\phi^{n+1})|&\leq 2C_1\|\Delta_h\sigma_\phi^{n+1}\|^2+3C_2\|\nabla\sigma_\phi^{n+1}\|^2+\frac{C}{C_2}h^{6q}\|\phi(t_{n+1})\|_{q+1,6}^6\\ &\quad+\frac{C}{C_2}h^{4q}\|\phi(t_{n+1})\|_{q+1,4}^4+\frac{C}{C_1}h^{2q+2}\|\phi(t_{n+1})\|_{q+1}^2.\end{aligned} \tag{3.24}$$

From (2.3), (3.1) and (3.20), one gets

$$\begin{aligned}&A\Delta t\big(\nabla(\sigma_w^{n+1}-\sigma_w^n),\nabla\sigma_\phi^{n+1}\big)=-A\Delta t(\sigma_w^{n+1}-\sigma_w^n,\Delta_h\sigma_\phi^{n+1})\\ &=-A\Delta t\big(\nabla(\sigma_\phi^{n+1}-\sigma_\phi^n),\nabla\Delta_h\sigma_\phi^{n+1}\big)+A\Delta t(\rho_w^{n+1}-\rho_w^n,\Delta_h\sigma_\phi^{n+1})\\ &\geq\frac{A\Delta t}{2}\big(\|\Delta_h\sigma_\phi^{n+1}\|^2-\|\Delta_h\sigma_\phi^n\|^2\big)-C_1\|\Delta_h\sigma_\phi^{n+1}\|^2-\frac{C\Delta t^3}{C_1}h^{2q+2}\int_{t_n}^{t_{n+1}}\|w_t\|_{q+1}^2\mathrm{d}t.\end{aligned} \tag{3.25}$$

Subsequently, we estimate the remaining terms on the right hand side of (3.23). Applying (2.3) and the Cauchy–Schwarz inequality yields

$$\big(\nabla(2\sigma_\phi^n-\sigma_\phi^{n-1}),\nabla\sigma_\phi^{n+1}\big)\leq\frac{\varepsilon^2}{4}\|\Delta_h\sigma_\phi^{n+1}\|^2+\frac{C}{\varepsilon^2}(\|\sigma_\phi^n\|^2+\|\sigma_\phi^{n-1}\|^2). \tag{3.26}$$

To analyze the second to the fifth terms, we resort to the Cauchy–Schwarz inequality and the Taylor expansion:

$$-(\delta_{\Delta t}^{n+1}\rho_\phi,\sigma_\phi^{n+1})\leq\frac{C_3}{2}\|\sigma_\phi^{n+1}\|^2+\frac{Ch^{2q+2}}{C_3\Delta t}\int_{t_{n-1}}^{t_{n+1}}\|\phi_t\|_{q+1}^2\mathrm{d}t, \tag{3.27}$$
$$(\mathcal{R}_1^{n+1},\sigma_\phi^{n+1})\leq\frac{C_3}{2}\|\sigma_\phi^{n+1}\|^2+\frac{C\Delta t^3}{C_3}\int_{t_{n-1}}^{t_{n+1}}\|\phi_{ttt}\|^2\mathrm{d}t, \tag{3.28}$$
$$A\Delta t(\mathcal{R}_2^{n+1},\nabla\sigma_\phi^{n+1})\leq C_2\|\nabla\sigma_\phi^{n+1}\|^2+\frac{C\Delta t^3}{C_2}\int_{t_n}^{t_{n+1}}\|\nabla w_t\|^2\mathrm{d}t, \tag{3.29}$$
$$(\mathcal{R}_3^{n+1},\nabla\sigma_\phi^{n+1})\leq C_2\|\nabla\sigma_\phi^{n+1}\|^2+\frac{C\Delta t^3}{C_2}\int_{t_{n-1}}^{t_{n+1}}\|\nabla\phi_{tt}\|^2\mathrm{d}t, \tag{3.30}$$
$$-\varepsilon^2(\rho_w^{n+1},\Delta_h\sigma_\phi^{n+1})\leq\frac{\varepsilon^2}{4}\|\Delta_h\sigma_\phi^{n+1}\|^2+C\varepsilon^2h^{2q+2}\|w(t_{n+1})\|_{q+1}^2. \tag{3.31}$$

Recall the $G-$norm introduced in [53]. Denote $\mathbf{p}^{k+1}=[\sigma_\phi^k,\sigma_\phi^{k+1}]^T$, and define $\|\mathbf{p}^{k+1}\|_{\mathbf{G}}^2\triangleq(\mathbf{p}^{k+1},\mathbf{G}\mathbf{p}^{k+1})$ where $\mathbf{G}=\begin{pmatrix}\frac{1}{2}&-1\\-1&\frac{5}{2}\end{pmatrix}$ is a symmetric positive definite matrix. Simple calculation gives

$$(\delta_{\Delta t}^{n+1}\sigma_\phi,\ \sigma_\phi^{n+1})=\frac{1}{2\Delta t}\big(\|\mathbf{p}^{n+1}\|_{\mathbf{G}}^2-\|\mathbf{p}^n\|_{\mathbf{G}}^2\big)+\frac{1}{4\Delta t}\|\sigma_\phi^{n+1}-2\sigma_\phi^n+\sigma_\phi^{n-1}\|^2. \tag{3.32}$$

Upon this, in combination with the above estimates for (3.23), one has

$$\begin{aligned}
&\frac{1}{2\Delta t}(\|\mathbf{p}^{n+1}\|_{\mathbf{G}}^2-\|\mathbf{p}^n\|_{\mathbf{G}}^2)+\frac{\varepsilon^2}{2}\|\Delta_h\sigma_\phi^{n+1}\|^2+\frac{A\Delta t}{2}(\|\Delta_h\sigma_\phi^{n+1}\|^2-\|\Delta_h\sigma_\phi^n\|^2)\\
&\le 3C_1\|\Delta_h\sigma_\phi^{n+1}\|^2+5C_2\|\nabla\sigma_\phi^{n+1}\|^2+C_3\|\sigma_\phi^{n+1}\|^2\\
&+\frac{C}{C_2}h^{6q}\|\phi(t_{n+1})\|_{q+1,6}^6+\frac{C}{C_2}h^{4q}\|\phi(t_{n+1})\|_{q+1,4}^4+\frac{C}{C_1}h^{2q+2}\|\phi(t_{n+1})\|_{q+1}^2\\
&+\frac{C\Delta t^3}{C_1}h^{2q+2}\int_{t_n}^{t_{n+1}}\|w_t\|_{q+1}^2\mathrm{dt}+\frac{Ch^{2q+2}}{C_3\Delta t}\int_{t_{n-1}}^{t_{n+1}}\|\phi_t\|_{q+1}^2\mathrm{dt}\\
&+\frac{C\Delta t^3}{C_3}\int_{t_{n-1}}^{t_{n+1}}\|\phi_{ttt}\|^2\mathrm{dt}+\frac{C\Delta t^3}{C_2}\int_{t_n}^{t_{n+1}}\|\nabla w_t\|^2\mathrm{dt}\\
&+\frac{C\Delta t^3}{C_2}\int_{t_{n-1}}^{t_{n+1}}\|\nabla\phi_{tt}\|^2\mathrm{dt}+C\varepsilon^2h^{2q+2}\|w(t_{n+1})\|_{q+1}^2+\frac{C}{\varepsilon^2}(\|\sigma_\phi^n\|^2+\|\sigma_\phi^{n-1}\|^2),
\end{aligned}\tag{3.33}$$

where $C_1,\ C_2,\ C_3$ can be arbitrary positive constants.

Next we turn to the case $n=0$. Similarly, taking $\varphi_h=\sigma_\phi^1$, $v_h=\varepsilon^2\Delta_h\sigma_\phi^1$ in (3.21)–(3.22) and adding the equations up, one gets

$$\begin{aligned}
&\Big(\frac{\sigma_\phi^1-\sigma_\phi^0}{\Delta t},\sigma_\phi^1\Big)+\varepsilon^2\|\Delta_h\sigma_\phi^1\|^2\\
&\le 2\hat{C}_1\|\Delta_h\sigma_\phi^1\|^2+3\hat{C}_2\|\nabla\sigma_\phi^1\|^2+2\hat{C}_3\|\sigma_\phi^1\|^2+\frac{C}{\varepsilon^2}\|\sigma_\phi^0\|^2\\
&+\frac{C}{\hat{C}_2}h^{6q}\|\phi(t_1)\|_{q+1,6}^6+\frac{C}{\hat{C}_2}h^{4q}\|\phi(t_1)\|_{q+1,4}^4+\frac{C}{\hat{C}_1}h^{2q+2}\|\phi(t_1)\|_{q+1}^2\\
&+\frac{Ch^{2q+2}}{\hat{C}_3\Delta t}\int_{t_0}^{t_1}\|\phi_t\|_{q+1}^2\mathrm{dt}+\frac{C\Delta t^2}{\hat{C}_3}\|\phi_{tt}\|_{L^\infty(0,T;L^2)}^2\\
&+\frac{C\Delta t^2}{\hat{C}_3}\|\Delta\phi_t\|_{L^\infty(0,T;L^2)}^2+C\varepsilon^2h^{2q+2}\|w\|_{L^\infty(0,T;H^{q+1})}^2.
\end{aligned}\tag{3.34}$$

Let $\hat{C}_3=\frac{1}{12\Delta t}$, and take $\hat{C}_2=\frac{\sqrt{\hat{C}_3\varepsilon^2}}{3}$, then $3\hat{C}_2\|\nabla\sigma_\phi^1\|^2\le\hat{C}_3\|\sigma_\phi^1\|^2+\frac{\varepsilon^2}{4}\|\Delta_h\sigma_\phi^1\|^2$. Moreover, take $\hat{C}_1=\frac{\varepsilon^2}{8}$, we have

$$\begin{aligned}
&\frac{\|\sigma_\phi^1\|^2}{4\Delta t}+\frac{\varepsilon^2}{2}\|\Delta_h\sigma_\phi^1\|^2\le\left(\frac{1}{2\Delta t}+\frac{C}{\varepsilon^2}\right)\|\sigma_\phi^0\|^2+C\left(\frac{h^{6q}}{\varepsilon}\|\phi\|_{L^\infty(0,T;W^{q+1,6})}^6\right.\\
&\left.+\frac{h^{4q}}{\varepsilon}\|\phi\|_{L^\infty(0,T;W^{q+1,4})}^4+\frac{h^{2q+2}}{\varepsilon^2}\|\phi\|_{L^\infty(0,T;H^{q+1})}^2\right)+Ch^{2q+2}\int_{t_0}^{t_1}\|\phi_t\|_{q+1}^2\mathrm{dt}\\
&+C\varepsilon^2h^{2q+2}\|w\|_{L^\infty(0,T;H^{q+1})}^2+C\Delta t^3\left(\|\phi_{tt}\|_{L^\infty(0,T;L^2)}^2+\|\Delta\phi_t\|_{L^\infty(0,T;L^2)}^2\right).
\end{aligned}\tag{3.35}$$

Thus we complete the estimate for $n=0$. For the same reason, let C_3 be a positive constant, take $C_1=\frac{\varepsilon^2}{24}$, $C_2=\frac{\sqrt{C_3\varepsilon^2}}{5}$, then $5C_2\|\nabla\sigma_\phi^{n+1}\|^2\le C_3\|\sigma_\phi^{n+1}\|^2+\frac{\varepsilon^2}{4}\|\Delta_h\sigma_\phi^{n+1}\|^2$. Multiplying equation (3.33) by $2\Delta t$, summing up for n and noticing that $\|\mathbf{p}^{n+1}\|_{\mathbf{G}}^2\ge\frac{1}{2}\|\sigma_\phi^{n+1}\|^2$ and $\|\mathbf{p}^1\|_{\mathbf{G}}^2=\frac{5}{2}\|\sigma_\phi^1\|^2$, one obtains

$$\begin{aligned}
&\frac{1-8\Delta tC_3}{2}\|\sigma_\phi^{n+1}\|^2+\frac{\varepsilon^2\Delta t}{4}\sum_{m=1}^n\|\Delta_h\sigma_\phi^{m+1}\|^2\\
&\le C\left(\frac{h^{6q}}{\varepsilon}\|\phi\|_{L^\infty(0,T;W^{q+1,6})}^6+\frac{h^{4q}}{\varepsilon}\|\phi\|_{L^\infty(0,T;W^{q+1,4})}^4+\frac{h^{2q+2}}{\varepsilon^2}\|\phi\|_{L^\infty(0,T;H^{q+1})}^2\right)\\
&+C\Delta t^4h^{2q+2}\int_{t_1}^{t_{n+1}}\|w_t\|_{q+1}^2\mathrm{dt}+Ch^{2q+2}\int_0^{t_{n+1}}\|\phi_t\|_{q+1}^2\mathrm{dt}\\
&+C\varepsilon^2h^{2q+2}\|w\|_{L^\infty(0,T;H^{q+1})}^2+C\Delta t^4\int_0^{t_{n+1}}\|\phi_{ttt}\|^2\mathrm{dt}+\frac{C\Delta t^4}{\varepsilon}\int_{t_1}^{t_{n+1}}\|\nabla w_t\|^2\mathrm{dt}\\
&+\frac{C\Delta t^4}{\varepsilon}\int_0^{t_{n+1}}\|\nabla\phi_{tt}\|^2\mathrm{dt}+\left(4C_3+\frac{C}{\varepsilon^2}\right)\Delta t\sum_{m=1}^n\|\sigma_\phi^m\|^2+\frac{5}{2}\|\sigma_\phi^1\|^2.
\end{aligned}\tag{3.36}$$

Combining (3.36) with (3.35) yields

$$\frac{1-8\Delta t C_3}{2}\|\sigma_\phi^{n+1}\|^2+\frac{\varepsilon^2\Delta t}{4}\sum_{m=1}^{n}\|\Delta_h\sigma_\phi^{m+1}\|^2 \le C_{\varepsilon,T}\left(h^{6q}+h^{4q}+h^{2q+2}+\Delta t^4\right)+C_\varepsilon\Delta t\sum_{m=1}^{n}\|\sigma_\phi^m\|^2. \tag{3.37}$$

Finally, let $C_3 \le \frac{1}{16}$, then the choice of $\Delta t < 1$ ensures that $\frac{1-8\Delta t C_3}{2} > \frac{1}{4}$, thus an application of the discrete Gronwall inequality gives

$$\|\sigma_\phi^{n+1}\|^2+\varepsilon^2\Delta t\sum_{m=1}^{n}\|\Delta_h\sigma_\phi^{m+1}\|^2 \le C_{\varepsilon,T}(h^{2q+2}+\Delta t^4). \tag{3.38}$$

Theorem 3.3. *Let (ϕ^n, w^n) and (ϕ_h^n, w_h^n) be the solution of (1.3) in the regularity class $\mathcal{C}_1$ and Problem 3.1 at time t_n respectively, then we have the following error estimate*

$$\|\phi^n-\phi_h^n\|+\left(\varepsilon^2\Delta t\sum_{m=1}^{n}\|w^m-w_h^m\|^2\right)^{\frac{1}{2}} \le C_{\varepsilon,T}(h^{q+1}+\Delta t^2), \tag{3.39}$$

for any $1 \le n \le N$, where $C_{\varepsilon,T}$ is a constant that only depends on ε and T.

Proof. Using the same arguments as in the last part of Theorem 2.2 and combining with estimate (3.38) make (3.39). □

Remark 3.2. In (3.32), the G-norm was adopted just like in [38,39,50] which is elegant and simple in the case of the uniform time step size, while it cannot be available for variable time steps. Recently in [51], the variable steps method was successfully applied to the CH equation, and the convergence analysis was firstly completed by a combination of energy estimates with a novel generalized discrete Gronwall type inequality. For the SS equation, it could be also applicable, and will be considered in our future work.

3.3. Precondition steepest decent solver

In this subsection, we describe a preconditioned steepest descent (PSD) algorithm for the fully discrete mixed finite element scheme, namely Problem 3.1, based on the theoretical framework in [40]. The fully discrete scheme (3.1) at time $n+1$ can be expressed as

$$\mathcal{N}(\phi^{n+1},\psi^{n+1})=f, \tag{3.40}$$

with

$$\mathcal{N}(\phi,\psi)=\begin{cases}\dfrac{3\phi-4\phi^n+\phi^{n-1}}{2\Delta t}-\nabla\cdot(|\nabla\phi|^2\nabla\phi)-(A\Delta t+\varepsilon^2)\Delta_h\psi+A\Delta t\Delta_h\psi^n\\ \psi+\Delta_h\phi\end{cases}, \tag{3.41}$$

$$f=\begin{cases}-\Delta_h(2\phi^n-\phi^{n-1})\\ 0\end{cases}. \tag{3.42}$$

Note that Eq. (3.40) can be regarded as a minimizer of energy

$$J(\phi)=\int_\Omega \frac{3}{2\Delta t}(\phi-\frac{4}{3}\phi^n+\frac{1}{3}\phi^{n-1})^2+\frac{1}{4}|\nabla\phi|^4+\frac{A\Delta t+\varepsilon^2}{2}|\Delta_h\phi|^2 d\mathbf{x} + \int_\Omega A\Delta t\Delta_h\phi^n\Delta_h\phi d\mathbf{x}+\int_\Omega \Delta_h(2\phi^n-\phi^{n-1})\phi d\mathbf{x}. \tag{3.43}$$

The main idea of the PSD solver is to use a linearized version of the nonlinear operator as a preconditioner, or in other words, as a metric for choosing the search direction [33]. A linearized version of the nonlinear operator $\mathcal{N}$ can be

$$\mathcal{L}(d,w):=\begin{pmatrix}\frac{3}{2\Delta t}d-(A\Delta t+\varepsilon^2)\Delta_h w\\ w+\Delta_h d\end{pmatrix}, \tag{3.44}$$

which is used to find an appropriate search direction. Given the current iterate $\phi^{n+1,k}$, the search direction can be computed by solving the equation $\mathcal{L}(d^k, w^k) = f - \mathcal{N}(\phi^{n+1,k}, \psi^{n+1,k})$, namely

$$\begin{cases} \left(\frac{3}{2\Delta t}d^k, v\right) + (A\Delta t + \varepsilon^2)(\nabla w^k, \nabla v) = \big(\nabla(2\phi^n - \phi^{n-1}), \nabla v\big) \\ \quad - \left(\frac{3\phi^{n+1,k} - 4\phi^n + \phi^{n-1}}{2\Delta t}, v\right) - (A\Delta t + \varepsilon^2)(\nabla\psi^{n+1,k}, \nabla v) \\ \quad + A\Delta t(\nabla\psi^n, \nabla v) - (|\nabla\phi^{n+1,k}|^2\nabla\phi^{n+1,k}, \nabla v), \\ (w^k, s) - (\nabla d^k, \nabla s) = 0. \end{cases} \tag{3.45}$$

With the current iterate and search direction on hand, the next iteration is updated as

$$\phi^{n+1,k+1} = \phi^{n+1,k} + \alpha_k d^k, \tag{3.46}$$

where $\alpha_k \in \mathbb{R}$ satisfies

$$\big(\mathcal{N}(\phi^{n+1,k+1}, \psi^{n+1,k+1}) - f, d^k\big) = 0.$$

The theoretical analysis in [40] suggests that the iteration sequence $\phi^{n+1,k}$ converges geometrically to the exact numerical solution ϕ^{n+1}, and the convergence rate is dependent on time step size Δt, independent of mesh grid size h.

Theorem 3.4. *Let $\phi^{n+1,k}$ be the sequence generated by (3.46) and ϕ^{n+1} the numerical solution of Problem 3.1 at time $n+1$. Then there exists a constant $C^* > 0$ such that*

$$e_k := J(\phi^{n+1,k}) - J(\phi^{n+1}) \le \left(1 - \frac{1}{2C^*}\right)^k e_0, \tag{3.47}$$

with $C^* = 1 + C_4(A\Delta t + \varepsilon^2)^{-\frac{3}{4}}(\frac{2\Delta t}{3})^{\frac{1}{4}}$, C_4 is a constant that only depends on Ω.

Remark 3.3. A geometric convergence rate is assured by Theorem 3.4. We observe that C^* depends on the values of Δt and ε, in other words, the PSD iteration convergence will accelerate as Δt decreases, and it will slow down as ε decreases.

The contraction estimate (3.47) is valid for the error of energy (3.43). Such a contraction estimate is not directly available for the error of the original phase variable $q_k := \phi^{n+1,k} - \phi^{n+1}$. However, we are still able to derive a geometric convergent estimate for q_k. The functional inequality is available

$$\begin{aligned} J(\phi^{n+1,k}) - J(\phi^{n+1}) &= \delta_\phi J(\phi^{n+1})(q_k) + \frac{1}{2}\delta_{\phi\phi}J(\theta)(q_k, q_k) = \frac{1}{2}\delta_{\phi\phi}J_h(\theta)(q_k, q_k) \\ &\ge \frac{3}{2\Delta t}\|q_k\|^2 + \frac{A\Delta t + \varepsilon^2}{2}\|\Delta_h q_k\|^2, \end{aligned} \tag{3.48}$$

where $\delta_\phi J(\phi)$, $\delta_{\phi\phi}J(\phi)$ are the first and second Gâteaux derivatives of $J(\phi)$, θ is in the line segment from $\phi^{n+1,k}$ to ϕ^{n+1} and $\delta_\phi J(\phi^{n+1}) = 0$ is applied in the second equality. As a direct consequence, we get

$$\frac{3}{2\Delta t}\|q_k\|^2 + \frac{A\Delta t + \varepsilon^2}{2}\|\Delta_h q_k\|^2 \le e_k \le e_0(C^*)^k \le r_{n+1}(C^*)^k, \tag{3.49}$$

where

$$\begin{aligned} r_{n+1} = &\frac{1}{6\Delta t}\|\phi^n - \phi^{n-1}\|^2 + \frac{1}{4}(\|\nabla\phi^n\|_{0,4}^4 - \|\nabla\phi^{n+1}\|_{0,4}^4) \\ &+ \frac{A\Delta t + \varepsilon^2}{2}(\|\Delta_h\phi^n\|^2 - \|\Delta_h\phi^{n+1}\|^2) + A\Delta t\big(\Delta_h\phi^n, \Delta_h(\phi^n - \phi^{n+1})\big) \\ &+ \big(\Delta_h(2\phi^n - \phi^{n-1}), \phi^n - \phi^{n+1}\big). \end{aligned}$$

The expression of r_{n+1} is derived by setting $\phi^{n+1,0} = \phi^n$. Then the geometric convergence analysis for the numerical error q_k, in both L^2 and H^2 norms immediately follows from (3.49). We also notice that $r_{n+1} = O(1)$.

Remark 3.4. The PSD algorithm for the fully discrete scheme (3.1) is slightly different from that proposed in [40]. Firstly, it is a mixed finite element version, secondly, for the choice of linearized operator $\mathcal{L}$, we just throw the nonlinear term $\nabla\cdot(|\nabla\phi|^2\nabla\phi)$ away rather than regarding $|\nabla\phi|^2$ as a constant, and the stability can be preserved by the existing stabilized term $A\Delta t\Delta_h(w - w^n)$.

Table 4.1
Global L^2 error at time $T = 1$, convergence rate and average iterations for the PSD solver with $\mathcal{P}_1$ element approximation. The parameters are given in the text, and the refinement path is taken to be $\Delta t = h/2$, thus the L^2 error is expected to be $\mathcal{O}(\Delta t^2) + \mathcal{O}(h^2) = \mathcal{O}(h^2)$ which is confirmed in the test.

h	$\Delta t = h/2$	$\|\phi(\cdot, T) - \phi_e(\cdot, T)\|$	Order	PSD iter
1/16	1/32	4.63333e−3	–	9
1/32	1/64	1.15934e−3	1.99875	7
1/64	1/128	2.90091e−4	1.99872	6
1/128	1/256	7.26815e−5	1.99685	5
1/256	1/512	1.83010e−5	1.98967	4

Table 4.2
L^2 error at time $T = 1$, convergence order for spatial approximation and average iterations for the PSD solver with $\mathcal{P}_2$ element approximation. The parameters are given in the text, and the refinement path is taken to be $\Delta t = h^2$, thus the L^2 error is expected to be $\mathcal{O}(\Delta t^2) + \mathcal{O}(h^3) = \mathcal{O}(h^3)$ which is confirmed in the test.

h	$\Delta t = h^2$	$\|\phi(\cdot, T) - \phi_e(\cdot, T)\|$	Order	PSD iter
1/16	$1/16^2$	5.00777e−5	–	7
1/32	$1/32^2$	6.24880e−6	3.00252	5
1/64	$1/64^2$	7.82013e−7	2.99831	4
1/128	$1/128^2$	9.81548e−8	2.99406	3

Table 4.3
L^2 error at time $T = 1$, convergence order for temporal approximation and average iterations for the PSD solver with $\mathcal{P}_2$ element approximation. The parameters are given in the text, and the refinement path is taken to be $\Delta t = h$, thus the L^2 error is expected to be $\mathcal{O}(\Delta t^2) + \mathcal{O}(h^3) = \mathcal{O}(h^2)$ which is confirmed in the test.

h	$\Delta t = h$	$\|\phi(\cdot, T) - \phi_e(\cdot, T)\|$	Order	PSD iter
1/16	1/16	5.09479e−5	–	14
1/32	1/32	7.80922e−6	2.70577	11
1/64	1/64	1.61276e−6	2.27564	9
1/128	1/128	3.69961e−7	2.12409	7

4. Numerical results

4.1. Convergence test

In this subsection, we test the convergence of the proposed numerical scheme. The computational domain is set as $\Omega = [0, 1]^2$, the final time is taken as $T = 1$, the artificial regularization parameter is given by $A = \frac{1}{16}$, and the surface diffusion coefficient is chosen as $\varepsilon^2 = 0.05$. In order to test the convergence rate, we have to add an artificial term on the right hand side to make the exact solution

$$\phi_e(x, y, t) = \cos(\pi x) \cos(\pi y) \sin(t). \tag{4.1}$$

For the spatial discretization, both the $\mathcal{P}_1$ and $\mathcal{P}_2$ elements are used with uniform meshes. To verify the optimal convergence order, we set the time step size $\Delta t = h/2$ for the $\mathcal{P}_1$ element case, thus at the final time $T = 1$, we expect an global error $\mathcal{O}(\Delta t^2) + \mathcal{O}(h^2) = \mathcal{O}(h^2)$ as $h \to 0$. As for the $\mathcal{P}_2$ element, we firstly set $\Delta t = h$ to check the second order approximation for the temporal discretization and then let $\Delta t = h^2$ to observe the spatial convergence order.

At each time level, we need a PSD solver to implement the numerical scheme. The corresponding results are displayed in Tables 4.1–4.3, from which we observe that the PSD iteration terminates in several steps. In addition, the convergence order is consistent with our theoretical analysis.

4.2. Complexity of the PSD iteration

In this subsection, we test the complexity of the PSD solver with the same parameters as in the previous subsection, except by taking the final time as $T = 0.32$. The dependence of PSD iteration on spatial mesh size h, time step size Δt and the value of ε are demonstrated in Table 4.4, from which we observe that the number of the PSD iteration increases obviously with an increasing value of Δt and a decreasing value of ε. These behaviors have confirmed the theoretical results (3.47), in terms of the dependence of the PSD iteration on the parameter Δt and ε. Besides, the choice of h does not affect the number of iteration, and this is consistent with the theoretical analysis.

Table 4.4
The dependence of the PSD iteration on different parameters h, ε and Δt.

Average PSD Iter	$h = 1/16$	$h = 1/32$	$h = 1/64$	$h = 1/128$	$h = 1/256$
$\Delta t = 0.01$ $\varepsilon^2 = 0.05$	3.94	3.94	3.97	3.97	3.97
Average PSD Iter	$\varepsilon^2 = 0.005$	$\varepsilon^2 = 0.01$	$\varepsilon^2 = 0.03$	$\varepsilon^2 = 0.05$	$\varepsilon^2 = 0.1$
$\Delta t = 0.01$ $h = 1/128$	5.25	4.75	4.13	3.97	3.75
Average PSD Iter	$\Delta t = 0.1$	$\Delta t = 0.05$	$\Delta t = 0.01$	$\Delta t = 0.005$	$\Delta t = 0.001$
$\varepsilon^2 = 0.05$ $h = 1/128$	7.81	5.63	3.97	3.61	2.96

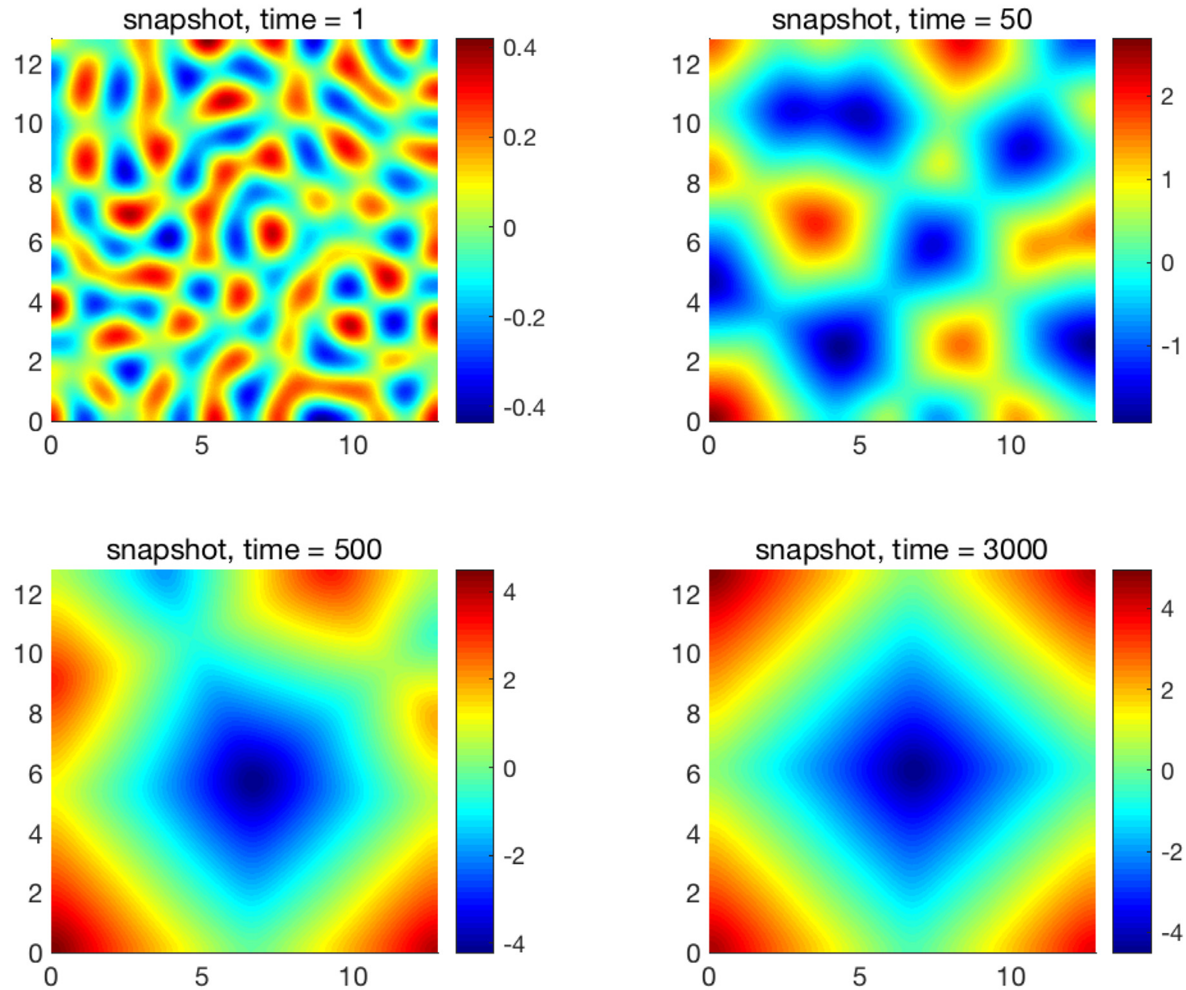

Fig. 4.1. Time snapshots of the evolution for the thin film epitaxial growth model with slope selection at $t = 1, 50, 500, 3000$. The parameters are $\Omega = [0, 12.8]^2$, $h = 12.8/128$, $t \in [0, 3000]$, $\varepsilon^2 = 0.05$, $\Delta t = 0.004$ for $t \in [0, 200]$, $\Delta t = 0.04$ for $t \in [200, 1000]$, $\Delta t = 0.08$ for $t \in [1000, 2000]$, $\Delta t = 0.15$ for $t \in [2000, 3000]$ and $A = \frac{1}{16}$.

4.3. Long time numerical simulation

In this subsection we test the energy decay property for the fully discrete scheme (3.1). Besides, the roughness of the height function is also investigated. The expression for the roughness of the height function is

$$R(\phi) = \sqrt{\frac{1}{|\Omega|}\int_\Omega \left(\phi(x,t) - \overline{\phi}(t)\right)^2 d\mathbf{x}}, \quad \text{with } \overline{\phi}(t) = \frac{1}{|\Omega|}\int_\Omega \phi(x,t) d\mathbf{x}. \tag{4.2}$$

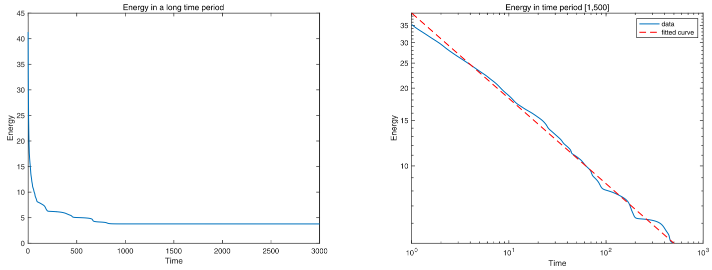

Fig. 4.2. The left panel: the plot of energy evolution. The right panel: the log–log plot of energy in time period [1,500]; The blue line represents the data obtained by numerical simulation while the dashed red line is a least square approximation. The fitted line has the form at^b with $a = 39.03,\ b = -0.33$.

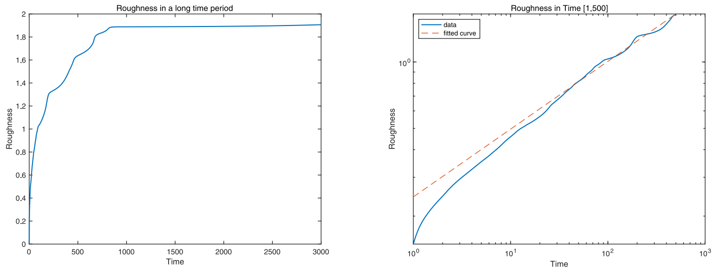

Fig. 4.3. The left panel: the plot of roughness evolution. The right panel: the log–log plot of roughness in time period [1,500]; The blue line represents the data obtained by numerical simulation while the dashed red line is a least square approximation. The fitted line has the form at^b with $a = 0.2444,\ b = 0.3074$.

Here we set the parameters as $\Omega = [0, 12.8]^2,\ t \in [0, 3000],\ \varepsilon^2 = 0.05,\ \Delta t = 0.004$ for $t \in [0, 200],\ \Delta t = 0.04$ for $t \in [200, 1000],\ \Delta t = 0.08$ for $t \in [1000, 2000]$, $\Delta t = 0.15$ for $t \in [2000, 3000]$ and $A = \frac{1}{16}$. The initial data for the simulation is randomly distributed in $(-0.05, 0.05)$. The snapshot figures of the phase variable at a sequence of time instants, $t = 1$, $t = 50$, $t = 500$ and $t = 3000$, are displayed in Fig. 4.1.

The evolution of energy and roughness is displayed in Figs. 4.2 and 4.3, respectively, and the numerical results have confirmed the approximate $t^{-1/3}$ energy decay rate and $t^{1/3}$ roughness growth rate (vs time) estimates [4].

5. Concluding remarks

In this paper, we have proposed and analyzed a mixed finite element method with modified second-order backward differentiation formula for solving the thin film epitaxy with slope selection equation. The energy stability has been established, and an optimal convergence rate $\mathcal{O}(h^{q+1} + \Delta t^2)$ has been proved. In addition, an efficient preconditioned steepest descent iterative algorithm has been used to solve the fully discrete system. The corresponding numerical tests have been undertaken to verify the theoretical analysis.

Acknowledgment

This work is supported in part by the grants NSFC, PR China 11671098, 91630309, a 111 project, PR China B08018 (W. Chen), NSF, USA DMS-1418689 (C. Wang). C. Wang also thanks the Key Laboratory of Mathematics for Nonlinear Sciences, Fudan University, for support during his visit. The authors would like to thank the anonymous reviewers for their valuable comments that improve this paper greatly.

References

[1] B. Li, High-order surface relaxation versus the Ehrlich-Schwoebel effect, Nonlinearity 19 (11) (2006) 2581–2603.
[2] B. Li, J. Liu, Thin film epitaxy with or without slope selection, European J. Appl. Math. 14 (2003) 713–743.
[3] B. Li, J. Liu, Epitaxial growth without slope selection: energetics, coarsening, and dynamic scaling, J. Nonlinear Sci. 14 (2004) 429–451.
[4] R. Kohn, X. Yan, Upper bound on the coarsening rate for an epitaxial growth model, Comm. Pure Appl. Math. 56 (2003) 1549–1564.
[5] S.M. Wise, C. Wang, J.S. Lowengrub, An energy-stable and convergent finite-difference scheme for the phase field crystal equation, SIAM J. Numer. Anal. 47 (3) (2009) 2269–2288.
[6] C. Xu, T. Tang, Stability analysis of large time-stepping methods for epitaxial growth models, SIAM J. Numer. Anal. 44 (4) (2006) 1759–1779.
[7] D. Li, Z. Qiao, T. Tang, Characterizing the stabilization size for semi-implicit Fourier-spectral method to phase field equations, SIAM J. Numer. Anal. 54 (2016) 1653–1681.

[8] C. Liu, J. Shen, X. Yang, Decoupled energy stable schemes for a phase-field model of two-phase incompressible flows with variable density, J. Sci. Comput. 62 (2) (2015) 601–622.
[9] R. Chen, G. Ji, X. Yang, H. Zhang, Decoupled energy stable schemes for phase-field vesicle membrane model, J. Comput. Phys. 302 (2015) 509–523.
[10] J. Shen, X. Yang, An efficient moving mesh spectral method for the phase-field model of two-phase flows, J. Comput. Phys. 228 (8) (2009) 2978–2992.
[11] A. Baskaran, Z. Hu, J.S. Lowengrub, C. Wang, S.M. Wise, P. Zhou, Energy stable and efficient finite-difference nonlinear multigrid schemes for the modified phase field crystal equation, J. Comput. Phys. 250 (2013) 270–292.
[12] A. Baskaran, J.S. Lowengrub, C. Wang, S.M. Wise, Convergence analysis of a second order convex splitting scheme for the modified phase field crystal equation, SIAM J. Numer. Anal. 51 (5) (2013) 2851–2873.
[13] L. Dong, W. Feng, C. Wang, S.M. Wise, Z. Zhang, Convergence analysis and numerical implementation of a second order numerical scheme for the three-dimensional phase field crystal equation, Comput. Math. Appl. 75 (6) (2018) 1912–1928.
[14] Z. Hu, S.M. Wise, C. Wang, J.S. Lowengrub, Stable and efficient finite-difference nonlinear-multigrid schemes for the phase-field crystal equation, J. Comput. Phys. 228 (15) (2009) 5323–5339.
[15] C. Wang, S.M. Wise, Global smooth solutions of the modified phase field crystal equation, Methods Appl. Anal. 17 (2010) 191–212.
[16] C. Wang, S.M. Wise, An energy stable and convergent finite-difference scheme for the modified phase field crystal equation, SIAM J. Numer. Anal. 49 (2011) 945–969.
[17] W. Chen, W. Feng, Y. Liu, C. Wang, S.M. Wise, A second order energy stable scheme for the Cahn-Hilliard-Hele-Shaw equation, Discrete Contin. Dyn. Syst. Ser. B 24 (1) (2019) 149–182.
[18] W. Chen, Y. Liu, C. Wang, S.M. Wise, An optimal-rate convergence analysis of a fully discrete finite difference scheme for Cahn-Hilliard-Hele-Shaw equation, Math. Comp. 85 (301) (2016) 2231–2257.
[19] C. Collins, J. Shen, S.M. Wise, An. efficient, An efficient energy stable scheme for the Cahn-Hilliard-Brinkman system, Commun. Comput. Phys. 13 (4) (2013) 929–957.
[20] A. Diegel, X. Feng, S.M. Wise, Convergence analysis of an unconditionally stable method for a Cahn-Hilliard-Stokes system of equations, SIAM J. Numer. Anal. 53 (2015) 127–152.
[21] A. Diegel, C. Wang, X. Wang, S.M. Wise, Convergence analysis and error estimates for a second order accurate finite element method for the Cahn-Hilliard-Navier–Stokes system, Numer. Math. 137 (3) (2017) 495–534.
[22] Y. Liu, W. Chen, C. Wang, S.M. Wise, Error analysis of a mixed finite element method for a Cahn-Hilliard-Hele-Shaw system, Numer. Math. 135 (3) (2017) 679–709.
[23] W. Chen, S. Conde, C. Wang, X. Wang, S.M. Wise, A linear energy stable scheme for a thin film model without slope selection, J. Sci. Comput. 52 (3) (2012) 546–562.
[24] W. Chen, W. Li, Z. Luo, C. Wang, X. Wang, A stabilized second order ETD multistep method for thin film growth model without slope selection, Math. Model. Numer. Anal. (2019) (in press).
[25] W. Chen, C. Wang, X. Wang, S.M. Wise, A linear iteration algorithm for energy stable second order scheme for a thin film model without slope selection, J. Sci. Comput. 59 (3) (2014) 574–601.
[26] K. Cheng, Z. Qiao, C. Wang, A third order exponential time differencing numerical scheme for no-slope-selection epitaxial thin film model with energy stability, J. Sci. Comput. 81 (1) (2019) 154–185.
[27] Y. Cheng, A. Kurganov, Z. Qu, T. Tang, Fast and stable explicit operator splitting methods for phase-field models, J. Comput. Phys. 303 (C) (2015) 45–65.
[28] H.G. Lee, J. Shin, J.Y. Lee, A second-order operator splitting Fourier spectral method for models of epitaxial thin film growth, J. Sci. Comput. 71 (3) (2017) 1303–1318.
[29] X. Li, Z. Qiao, H. Zhang, Convergence of a fast explicit operator splitting method for the epitaxial growth model with slope selection, SIAM J. Numer. Anal. 55 (1) (2017) 265–285.
[30] X. Yang, J. Zhao, Q. Wang, Numerical approximations for the molecular beam epitaxial growth model based on the invariant energy quadratization method, J. Comput. Phys. 333 (2017) 104–127.
[31] L. Chen, J. Zhao, X. Yang, Regularized linear schemes for the molecular beam epitaxy model with slope selection, Appl. Numer. Math. 128 (2018) 139–156.
[32] Q. Cheng, J. Shen, X. Yang, Highly efficient and accurate numerical schemes for the epitaxial thin film growth models by using the SAV approach, J. Sci. Comput. 78 (3) (2019) 1–21.
[33] W. Feng, C. Wang, S.M. Wise, Z. Zhang, A second-order energy stable backward differentiation formula method for the epitaxial thin film equation with slope selection, Numer. Methods Partial Differential Equations 34 (6) (2018) 1975–2007.
[34] J. Shen, C. Wang, X. Wang, S.M. Wise, Second-order convex splitting schemes for gradient flows with Ehrlich-Schwoebel type energy: application to thin film epitaxy, SIAM J. Numer. Anal. 50 (2012) 105–125.
[35] C. Wang, X. Wang, S.M. Wise, Unconditionally stable schemes for equations of thin film epitaxy, Discrete Contin. Dyn. Syst. 28 (2010) 405–423.
[36] W. Chen, Y. Wang, A mixed finite element method for thin film epitaxy, Numer. Math. 122 (4) (2012) 771–793.
[37] Z. Qiao, T. Tang, H. Xie, Error analysis of a mixed finite element method for the molecular beam epitaxy model, SIAM J. Numer. Anal. 53 (1) (2015) 184–205.
[38] W. Li, W. Chen, C. Wang, Y. Yan, R. He, A second order energy stable linear scheme for a thin film model without slope selection, J. Sci. Comput. 76 (3) (2018) 1905–1937.
[39] W. Chen, Y. Zhang, W. Li, Y. Wang, Y. Yan, Optimal convergence analysis of a second order scheme for a thin film model without slope selection, J. Sci. Comput. 80 (3) (2019) 1716–1730.
[40] W. Feng, A.J. Salgado, C. Wang, S.M. Wise, Preconditioned steepest descent methods for some nonlinear elliptic equations involving p-laplacian terms, J. Comput. Phys. 334 (2017) 45–67.
[41] J.W. Cahn, J.E. Hilliard, Free energy of a non-uniform system. I. interfacial free energy, J. Chem. Phys. 28 (2) (1958) 258–267.
[42] J. Shen, X. Yang, Numerical approximations of Allen-Cahn and Cahn-Hilliard equations, Discrete Contin. Dyn. Syst. Ser. A 28 (4) (2010) 1669–1691.
[43] A. Christlieb, J. Jones, K. Promislow, B. Wetton, M. Willoughby, High accuracy solutions to energy gradient flows from material science models, J. Comput. Phys. 257 (1) (2014) 193–215.
[44] W. Feng, Z. Guan, J.S. Lowengrub, C. Wang, S.M. Wise, Y. Chen, A uniquely solvable, energy stable numerical scheme for the functionalized Cahn-Hilliard equation and its convergence analysis, J. Sci. Comput. 76 (3) (2018) 1938–1967.
[45] R.A. Adams, J.J.F. Fournier, Sobolev Spaces, second ed., Academic press, Singapore, 2003.
[46] V. Thomée, Galerkin Finite Element Methods for Parabolic Problems, vol. 1054, Springer, 1984.
[47] V. Girault, P.A. Raviart, Finite Element Methods for Navier–Stokes Equations: Theory and Algorithms, Springer-Verlag, Berlin Heidelberg, 1986.
[48] Y. Yan, W. Li, W. Chen, Y. Wang, Optimal convergence analysis of a mixed finite element method for fourth-order elliptic problems, Commun. Comput. Phys. 24 (2) (2018) 510–530.

[49] K. Cheng, W. Feng, C. Wang, S.M. Wise, An energy stable fourth order finite difference scheme for the Cahn-Hilliard equation, J. Comput. Appl. Math. 362 (2019) 574–595.
[50] Y. Yan, W. Chen, C. Wang, S.M. Wise, A second-order energy stable BDF numerical scheme for the Cahn-Hilliard equation, Commun. Comput. Phys. 23 (2018) 572–602.
[51] W. Chen, X. Wang, Y. Yan, Z. Zhang, Second order BDF numerical scheme with variable steps for the Cahn-Hilliard equation, SIAM J. Numer. Anal. 57 (1) (2019) 495–525.
[52] D. Li, Z. Qiao, On second order semi-implicit Fourier spectral methods for 2D Cahn-Hilliard equations, J. Sci. Comput. 70 (1) (2017) 301–341.
[53] W. Chen, M. Gunzburger, D. Sun, X. Wang, Efficient and long-time accurate second-order methods for the Stokes-Darcy system, SIAM J. Numer. Anal. 51 (5) (2013) 2563–2584.